

CHAPTER 245

COMBINED CONVECTION-DIFFUSION MODELLING OF SEDIMENT ENTRAINMENT

by

Peter Nielsen

Abstract

A new, quantitative framework is presented for the modelling of suspended sediment concentration distributions. It accounts for large scale mixing (convection) as well as small scale mixing. The small scale mixing is modelled in terms of gradient diffusion as usual. It is shown how the new, combined convection-diffusion model can explain the different $\bar{c}(z)$ -distributions of different sediment sizes in the same flow. Also, the dependence of the $\bar{c}(z)$ -distribution shape on wave period and sediment settling velocity is explained for oscillatory flow over ripples. It is shown that individual Fourier components of $c_n(z,t)$ behave differently in diffusion dominated and in convection dominated flows. This makes it possible to determine the dominant entrainment mechanism (convection or diffusion) on the basis of concentration time series taken simultaneously at different levels.

1. Introduction

Experimental data calls for a new description of the distribution of suspended sediment. That is, the traditional gradient diffusion model is inadequate as a description of many natural suspension processes.

Gradient diffusion is suited only as a description for processes where the mixing length l_m is small compared to the overall scale. It cannot describe details on a scale comparable or smaller than l_m , see Figure 1.

Some of the natural processes which involve large scale mixing mechanisms are: Entrainment of sand from rippled beds, lifting of sand straight from the bed to the surface behind plunging breakers, entrainment by turbulent bursts in sheet flow, entrainment by the obliquely descending vortices of Nadaoka et al (1988), and from steady streams, entrainment by the vortices which are formed behind dunes and subsequently carry sand to the surface.

Department of Civil Engineering, The University of Queensland, St Lucia,
Australia 4072, fax +61 7 365 4599.

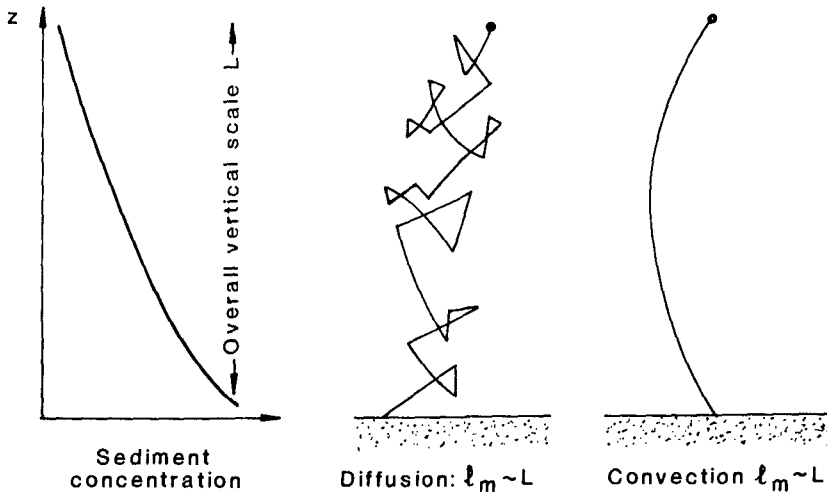


Figure 1: A concentration profile with overall scale L may be generated by either gradient diffusion ($l_m < L$) or convective entrainment ($l_m \sim L$), but usually it will be due to a mixture of both.

These processes require a different modelling framework than gradient diffusion.

The quantitative framework for the combined convection-diffusion process is briefly derived in Sections 3 and 4. The main new ingredient here is the expression for the convective upward flux proposed by Nielsen (1991).

Section 5 then discusses the shape of the distributions of time-averaged concentrations $\bar{c}(z)$. A single shape parameter S is defined with which variation in shape of the $\bar{c}(z)$ -profiles with wave period and sediment settling velocity can be explained.

The behaviour of the time dependent (harmonic) components $c_n(z,t)$ of the concentration is discussed in Section 6. It is shown how the relative importance of convective versus diffusive mixing is indicated by simultaneous concentration time series from different elevations.

3. Quantification of the convective entrainment flux

Most natural suspension processes involve mixing on different scales, see Figure 1, and mechanisms with large mixing lengths l_m compared with the overall scale, require a different mathematical framework than gradient diffusion. A quantitative description for the large scale ($l_m \sim L$) mixing mechanisms is suggested as outlined in Figure 2.

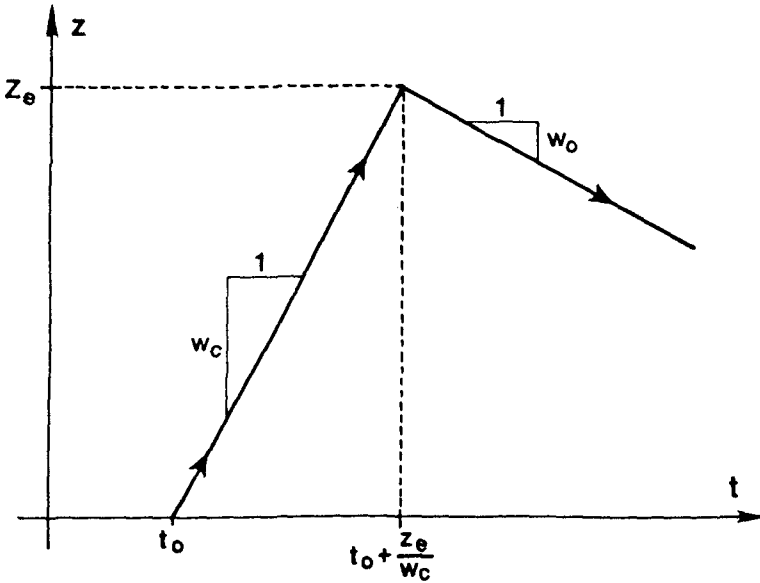


Figure 2: Sand which is entrained from the bed at time t_0 is assumed to travel upwards with speed w_c . Not all of the sand will reach the same level. The distribution of entrainment levels z_e is given by $F(z) = P\{z_e > z\}$. After reaching its entrainment level z_e at time $t_0 + z_e/w_c$, a sand particle is assumed to settle out with its still water settling velocity w_0 . During the settling process it may be affected by small scale mixing (diffusion).

A quantitative description of the convective, upward sediment flux $q_c(z,t)$ in accordance with Figure 2, has been derived by Nielsen (1991,1992). He suggested the form

$$q_c(z,t) = p\left(t - \frac{z}{w_c}\right) F(z) \quad (1)$$

where $p(t)$ is the amount of sand which is picked up from the bed at time t .

4. Continuity equation for the combined process

The continuity equation for the combined process, i.e., the equation which expresses the conservation of sand in the combined convection diffusion process is

$$\frac{\partial c}{\partial t} = w_0 \frac{\partial c}{\partial z} - \frac{\partial q_c}{\partial z} - \frac{\partial q_D}{\partial z} \quad (2)$$

which with the expression (1) inserted for the convective upward flux, and with

the upward diffusive flux $q_D = -\epsilon_s \frac{\partial c}{\partial z}$ becomes

$$\frac{\partial c}{\partial t} = w_o \frac{\partial c}{\partial z} + \frac{1}{w_c} p'(t - \frac{z}{w_c}) F(z) - p(t - \frac{z}{w_c}) F'(z) + \frac{\partial}{\partial z} (\epsilon_s \frac{\partial c}{\partial z}) \quad (3)$$

or

$$\frac{\partial c}{\partial t} - w_o \frac{\partial c}{\partial z} - \frac{\partial}{\partial z} (\epsilon_s \frac{\partial c}{\partial z}) = \frac{1}{w_c} p'(t - \frac{z}{w_c}) F(z) - p(t - \frac{z}{w_c}) F'(z) \quad (4)$$

from which we see that the homogeneous equation is the usual diffusion equation, while the convective flux enters only through the forcing terms.

4. The shape of the $\bar{c}(z)$ -profiles

The inadequacy of pure gradient diffusion as a universal model for sediment suspension becomes particularly evident when one considers the distributions of different grain sizes in the same flow. An example is shown in Figure 3.

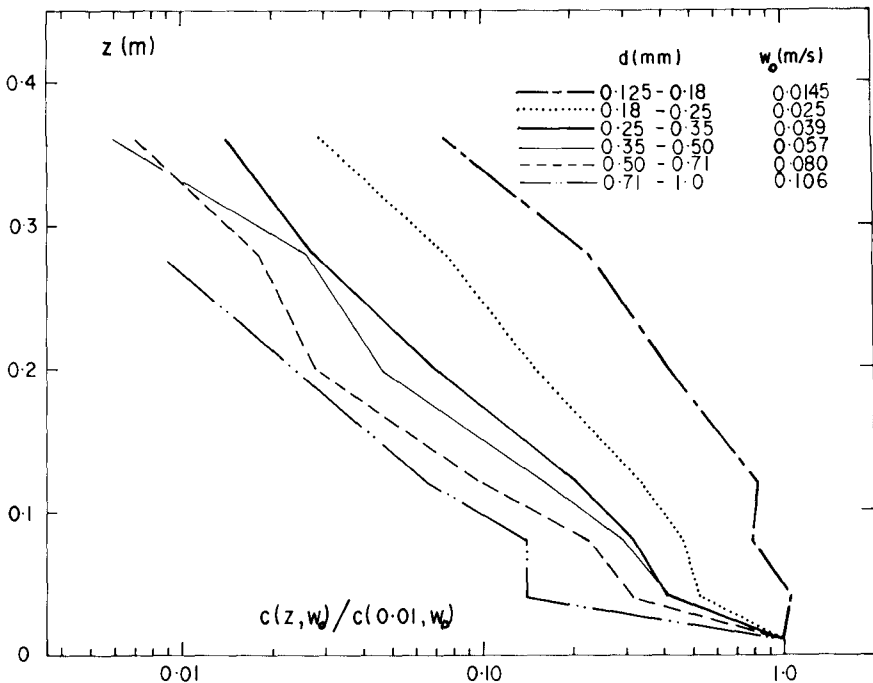


Figure 3: Normalised distributions of different sand sizes in the same flow (oscillatory flow over ripples). The data was obtained by sieving suction samples from each elevation. Data from Nielsen (1983).

The interesting thing about these profiles is that they do not have the same shape. In this case, the fine sand shows typically upward convex profiles while the coarse sand shows upward concave profiles. Such differences between different sand sizes (different settling velocities w_o) cannot be explained within the gradient diffusion framework. If the concentration profiles had been a result of pure gradient diffusion with diffusivity $\epsilon_s(z)$, they would have had the mathematical form

$$\ln \frac{\bar{c}}{C_o} = -w_o \int_0^z \frac{dz}{\epsilon_s} \quad (5)$$

where $C_o = \bar{c}(o)$.

This shows that the profiles for different sand sizes would have similar shapes when plotted as in Figure 3, the role of the settling velocity w_o would be only to tilt the profiles towards the left.

The same picture as Figure 3 was presented by the natural-ripple-data from a subsequent laboratory study of McFetridge & Nielsen (1985).

Another observation which underlines the need for a new distribution model is that time averaged concentration profiles over rippled beds under waves tend to change shape from upward convex to upward concave with increasing wave period. Examples of this are shown in Figure 4.

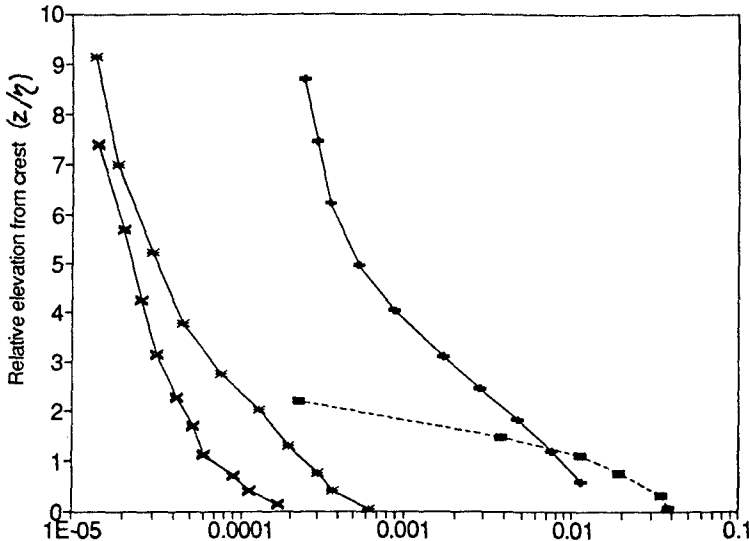


Figure 4: Time averaged concentration profiles over rippled beds in an oscillating water tunnel. For the shortest periods, the \bar{c} -profiles are upward convex (at least for the first 4 ripple heights). With increasing T , they become more and more upward concave. $d_{50}=0.21mm$ in all of the experiments. \blacksquare : $T=1s$, $U_{max}=0.5m/s$, $+$: $T=2s$, $U_{max}=0.5s$, $*$: $T=4s$, $U_{max}=0.3m/s$, x : $T=10s$, $U_{max}=0.3m/s$. Data from Bosman (1982) and Ribberink & Al-Salem (1989).

This change of shape of the $\bar{c}(z)$ -profiles with wave period is difficult to explain within the gradient diffusion framework. The different shapes for $\bar{c}(z)$ would, in that framework, indicate different distributions of the diffusivity $\varepsilon_s(z)$. That is however an unlikely explanation, in so far as $\varepsilon_s(z)$ should be closely related to the eddy viscosity and hence similar from experiment to experiment, because the flow conditions were rather similar.

Furthermore, a similar set of concentration profiles measured over flat beds (Horikawa et al 1982) show the same gradual change of shape with increasing period, see Nielsen (1992) p271.

We shall see that both the change from upward convex to upward concave for sediments with increasing settling velocity in the same flow and the analogous change for the same sand in flows with increasing periods can be modelled by the combined convection diffusion model. The shape differences are shown to be consequences of different relative importance of diffusive (small scale) and convective (large scale) mixing, and this is quantified in terms of the shape parameter S . The shape parameter is found to follow the rough, general rule

$$S \sim \frac{w_o T}{\sqrt{A} r} \quad (6)$$

where A is the wave induced particle semi excursion just above the boundary layer and r is the bed roughness.

When S is small, the \bar{c} -profiles tend to be upward convex, for large S they tend to be upward concave.

The derivation of the form of the shape parameter (Nielsen 1992, p 249) is based on the solution to the time-averaged version

$$w_o \bar{c} + \varepsilon_s \frac{d\bar{c}}{dz} = \bar{p} F(z) \quad (7)$$

of the continuity equation (3) in the simple case where ε_s is a constant and $F(z) = \exp[-z/L]$. In that case the time averaged concentration is given by

$$\bar{c}(z) = \frac{\bar{p}}{w_o} \left\{ \frac{1}{1 - \varepsilon_s/w_o L} e^{-z/L} + \left(1 - \frac{1}{1 - \varepsilon_s/w_o L}\right) e^{-w_o z/\varepsilon_s} \right\}, \quad \varepsilon_s/w_o L \neq 1. \quad (8)$$

This solution shows that the relative importance of the diffusion solution (the last term) and the convection solution (the first term) is measured by the ratio $\varepsilon_s/w_o L$ which may be seen as the ratio between the vertical scale ε_s/w_o of the pure diffusion solution and that (L) of the pure convection solution. The inverse of this ratio is the shape parameter :

$$S = \frac{w_o L}{\epsilon_s} \quad (9)$$

To express the shape parameter in terms of basic flow parameters it is then noted that oscillatory boundary layers over rippled beds usually have a structure which is analogous to that of laminar oscillatory flow over a flat plate. That is, the eddy viscosity is constant, and its value is $\nu_t = 0.5 \omega z_1^2$ where $z_1 = 0.09 \sqrt{rA}$, cf Nielsen (1992) p 40. Hence, assuming that ϵ_s is proportional to ν_t and that the convective length scale L is proportional to z_1 we are lead to the formula (6) which agrees with the observations in Figures 3 and 4. That is, in both cases, the transition from upward convex to upward concave profiles happens with increasing values of S .

It is interesting to note that experiments with suspensions of limited amounts of sand over artificial, fixed ripples give less pronounced $\bar{c}(z)$ -shape differences between coarse and fine sand fractions. Such experiments were reported by McFetridge & Nielsen (1985) and by van de Graff (1988). In the fixed-ripple-experiments, the $\bar{c}(z)$ -profiles agree more closely with the gradient diffusion model in the sense of Equation (5). It is believed to be due to the fact that when the sand supply at the bed is limited, the convective entrainment mechanism is less important. Most of the sand stays in suspension rather than being continually picked up and resuspended by the travelling lee vortices. The limiting case in this respect is pure wash load which is hence expected to obey the diffusion equation very closely.

5. Time dependent concentrations in pure diffusion

The time dependent diffusion equation

$$\frac{\partial c}{\partial t} - w_o \frac{\partial c}{\partial z} - \frac{\partial}{\partial z} (\epsilon_s \frac{\partial c}{\partial z}) = 0 \quad (10)$$

which emerges from Equation (4) when the convective entrainment flux is zero, with the boundary conditions

$$\begin{aligned} -\epsilon_s \frac{\partial c}{\partial z} &= p(t) \quad \text{for } z = 0 \\ c(z,t) &\rightarrow 0 \quad \text{for } z \rightarrow \infty \end{aligned} \quad (11)$$

was solved by Nielsen et al (1978). The solution is in the form of a Fourier series and based on separation of the variables. Each concentration component $c_n(z,t)$ which is generated by the corresponding component $p_n(t) = P_n e^{in\omega t}$ of the pickup function was found to have the form

$$c_n(z,t) = \frac{P_n}{w_o \alpha_n} e^{-\alpha_n \frac{w_o z}{\epsilon_s}} e^{in\omega t} \quad (12)$$

where

$$\alpha_n = \frac{1}{2} + \sqrt{\frac{1}{4} + i \frac{n\omega \epsilon_s}{w_o^2}} \tag{13}$$

Alternatively Equation (12) may be written

$$c_n(z,t) = \frac{P_n}{w_o |\alpha_n|} e^{-Re\{\alpha_n\} \frac{w_o z}{\epsilon_s}} \cos(n\omega t - Arg\{\alpha_n\} - Im\{\alpha_n\} \frac{w_o z}{\epsilon_s}) \tag{14}$$

or with a slight rearrangement of the phase of the cosine function

$$c_n(z,t) = \frac{P_n}{w_o |\alpha_n|} e^{-Re\{\alpha_n\} \frac{w_o z}{\epsilon_s}} \cos \left[n\omega \left(t - \frac{Im\{\alpha_n\} w_o}{n \omega \epsilon_s} z \right) - Arg\{\alpha_n\} \right]$$

which shows that in a diffusion process with constant diffusivity, a concentration wave with radian frequency $n\omega$ travels upwards with speed $w_n = \frac{n \omega \epsilon_s}{w_o Im\{\alpha_n\}}$. The behaviour of the solution (14) is illustrated in Figure 5 for the case of $p(t) \sim w_o \cos^6(\omega t/2)$.

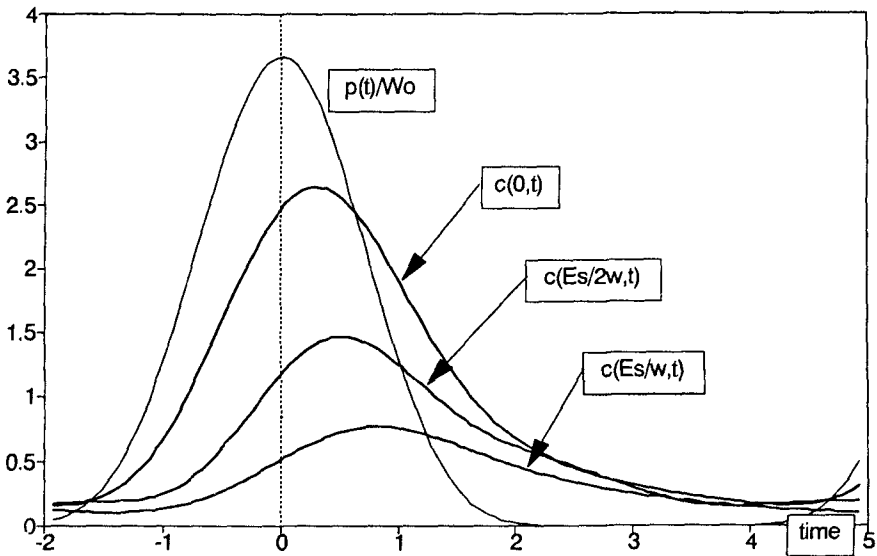


Figure 5: Sediment concentrations at different levels ($0, \frac{\epsilon_s}{2 w_o}$ and $\frac{\epsilon_s}{w_o}$) generated by the shown, periodic pickup function and pure gradient diffusion with constant diffusivity and $\omega \epsilon_s / w_o^2 = 1$

6. Time dependent concentrations in pure convection

For the case of purely convective entrainment we set $\epsilon_s = 0$ in Equation (4) and get

$$\frac{\partial c}{\partial t} - w_o \frac{\partial c}{\partial z} = \frac{1}{w_c} p'(t - \frac{z}{w_c}) F(z) - p(t - \frac{z}{w_c}) F'(z) \quad (15)$$

For the simple case of $F(z) = \exp(-z/L)$ this equation has a Fourier series solution, which corresponds to (12), with

$$c_n(z,t) = C_n e^{-\beta_n z/L} e^{in\omega t} \quad (16)$$

where

$$C_n = \frac{P_n}{w_o} \frac{\beta_n}{\beta_n + i \frac{n\omega L}{w_o}} \quad \text{and} \quad \beta_n = 1 + i \frac{n\omega L}{w_c} \quad (17)$$

cf Nielsen (1992) p 240. In analogy with (14) this solution can be written as

$$c_n(z,t) = |C_n| e^{-z/L} \cos[n\omega(t - z/w_c) + \text{Arg}\{C_n\}] \quad (18)$$

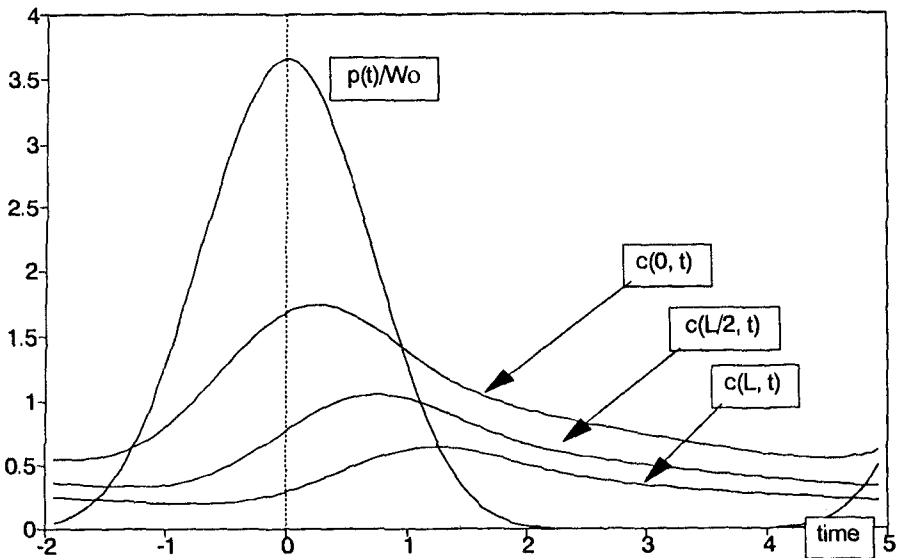


Figure 6: Sediment concentrations at different levels generated by the shown pickup function and purely convective entrainment. $F(z) = \exp(-z/L)$ and $\omega L/w_c = 1$.

This expression illustrates that all the harmonics of the pure convection solution decay at the same rate (as $F(z)$ in general, and as $\exp(-z/L)$ in this particular case), and that all time lags grow at the same rate with z . Compared with the diffusion case, this corresponds to a greater shape similarity between time series at different elevations for the convective case. The nature of the convection solution is illustrated in Figure 6 for the case of $p(t) \sim w_o \cos^6(\omega t/2)$ (same as for the diffusion solution in Figure 5).

7. Comparison with measured time series

Consider the situation where simultaneous time series $c(z_i,t)$ have been measured at a number of levels, and one wishes to infer the nature of the sediment entrainment process.

Before such an analysis is undertaken using the framework above one should note, that what has been measured by a point (or line) sensor and what is modelled above as $c(z_i,t)$ are not conceptually identical. The model assumes horizontal uniformity while the sensor samples from a spotted carpet of concentrations $c(x,y,z_i,t)$ which move back and forth with the waves. Thus, some of the time variation seen by the sensor is not modelled, and is indeed, not a feature of the horizontally averaged concentration $c(z_i,t)$. If the measurements have been taken close to a bed with strong topographical features the difference may be very significant. The problem may be amended (at least in part) by averaging over several sensors in the same horizontal plane or by using line sensors which average over one or more bedform lengths.

Assume now that concentration time series $c(z_i,t)$ have been measured by such an array of sensors that the abovementioned "spotted carpet effect" is neutralised, and that that the corresponding Fourier series have been obtained

$$\begin{aligned}
 c(z_i,t) &= \sum_0^\infty c_n(z_i,t) = \bar{c}(z_i) + \sum_{n=1}^\infty A_{i,n} \cos n\omega t + B_{i,n} \sin n\omega t \\
 &= \bar{c}(z_i) + \sum_1^\infty R_{i,n} \cos(n\omega t - \varphi_{i,n})
 \end{aligned}
 \tag{19}$$

where $R_{i,n} = \sqrt{A_{i,n}^2 + B_{i,n}^2}$ and $\varphi_{i,n} = \tan^{-1} \left(\frac{B_{i,n}}{A_{i,n}} \right)$.

First consider the possibilities of deriving information about ϵ_s , \bar{p} and $F(z)$ from the time averaged concentrations. The time-averaged continuity equation (7) can, if $\bar{c}(z)$ and w_o are known, be seen as having two unknowns namely $\epsilon_s(z)$ and $\bar{p}F(z)$. Thus, $\epsilon_s(z)$ and $\bar{p}F(z)$ cannot be determined from this equation alone. Additional information is needed. Such information can be sought along different lines.

Firstly, it may be that $\epsilon_s(z)$ can be inferred from knowledge about the

eddy viscosity ν_t . Indeed, one of the benefits of the combined convection diffusion model is that one should be able to assume identity between diffusivity and eddy viscosity.

Alternatively, if concentration profiles $\bar{c}_1(z)$ and $\bar{c}_2(z)$ of two different sand sizes with settling velocities w_1 and w_2 are known, we have at each level two equations (two versions of (7)) for finding the two unknowns $\epsilon_s(z)$ and $\bar{p}F(z)$. Unfortunately, such detailed datasets are rare at present.

Thirdly, as pointed out by Nielsen (1992) p 248, $\bar{p}F(z)$ may be inferred from the shape of $\bar{c}(z)$ alone for very coarse sand fractions. This is done simply by neglecting the second term in Equation (7).

Most of the available data on suspended sediment concentrations contain too little detail for the analysis outlined above. Usually, the measured concentrations are compounded by a fairly wide distribution of grain sizes and no information is available about the contributions from individual, narrow size fractions. Furthermore, much of the time series data obtained with optical or acoustical instruments suffer from uncertainty about the absolute magnitude of the concentrations.

However, some information can be extracted about the nature of the entrainment process even from such data. Assume that Fourier series of the form (19) have been obtained from at least two different levels and that the settling velocity distribution of the suspended material is narrow. Then the phase shifts and magnitudes of different Fourier components will show quite different developments in the two cases of pure gradient diffusion and purely convective entrainment.

It may be seen from the expressions (12) and (13) that the magnitudes of different Fourier components decay at different rates in a pure diffusion process with constant diffusivity. The decay rates are given by

$$\frac{d \ln|c_n|}{dz} = -\text{Re}\{\alpha_n\} \frac{w_0}{\epsilon_s} \quad (20)$$

which is an increasing function of the frequency $n\omega$. In contrast, in the case of purely convective entrainment, all components decay at the same rate, namely as $F(z)$. For $F(z) = \exp(-z/L)$ this means

$$\frac{d \ln|c_n|}{dz} = -1/L \quad \text{for all } n \quad (21)$$

The growth of the phase lags $\varphi_n(z)$ are also different for the two types of processes. For the gradient diffusion process with constant diffusivity, Equation (14) tells us that

$$\frac{d \varphi_n}{dz} = -\text{Im}\{\alpha_n\} \frac{w_0}{\epsilon_s} \quad (22)$$

while Equation (16) for the convection process with $F(z) = \exp(-z/L)$ gives

$$\frac{d \varphi_n}{dz} = - \text{Im}\{\beta_n\} \frac{1}{L} = - \frac{n\omega}{w_c} \tag{23}$$

corresponding to the same time lag for all components as was also indicated by Equation (18).

If relative increments

$$Y = \frac{\varphi_n(z_i) - \varphi_n(z_j)}{\ln \bar{c}(z_j) - \ln \bar{c}(z_i)} \tag{24}$$

of the phase shifts φ_n are plotted against the relative increments

$$X = \frac{\ln |c_n(z_j)| - \ln |c_n(z_i)|}{\ln \bar{c}(z_j) - \ln \bar{c}(z_i)} = \frac{\ln R_{j,n} - \ln R_{i,n}}{\ln \bar{c}(z_j) - \ln \bar{c}(z_i)} \tag{25}$$

of $\ln |c_n|$ as in Figure 7, the result for a pure diffusion process will trace the hyperbola branch $Y = \sqrt{X^2 - 1}$, $x > 0$ which is the locus for α_n in the complex plane. For the pure convection case, the points will trace the vertical line $X = 1$, $Y > 0$, which is the locus of β_n .

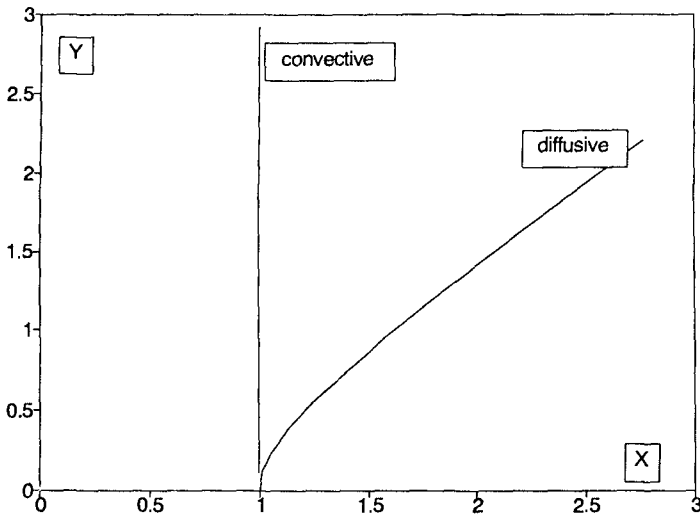


Figure 7: The relative decay rates (X) and phase lag increments (Y) defined by (25) and (24) correspond respectively to the parameters α_n in pure diffusion with constant ϵ_s and, to β_n for purely convective entrainment with $F(z) = \exp(-z/L)$. For details about α_n see Nielsen (1979), p 131.

Finally, we note that information about the convective entrainment velocity w_c may be found simply by considering the time difference between the occurrence of identifiable peaks at different levels, cf Equation (18). If a peak arrives at z_i at time t_i and at z_j at time t_j , the corresponding w_c in a purely convective entrainment process is given by

$$w_c = \frac{z_j - z_i}{t_j - t_i} \tag{26}$$

In contrast to the convective entrainment process considered above, the upward propagation speed of a concentration wave in a diffusive medium is frequency dependent as mentioned in connection with Equation (14). For constant diffusivity, the speed w_n of a concentration wave with frequency $n\omega$ is given by

$$w_n = \frac{n\omega\epsilon_s/w_0}{\text{Im}\{\alpha_n\}} \tag{27}$$

or

$$\frac{w_n}{w_0} = \frac{n\omega\epsilon_s/w_0^2}{\text{Im}\{\alpha_n\}} = \frac{n\omega\epsilon_s/w_0^2}{\text{Im}\left\{\frac{1}{2} + \sqrt{\frac{1}{4} + i\frac{n\omega\epsilon_s}{w_0^2}}\right\}} \tag{28}$$

the behaviour of which is illustrated in Figure 8. In the limit of $w_0 \rightarrow 0$ i.e. for neutrally buoyant sediments or momentum, the value of w_n is simply $\sqrt{2 n \omega \epsilon_s}$.

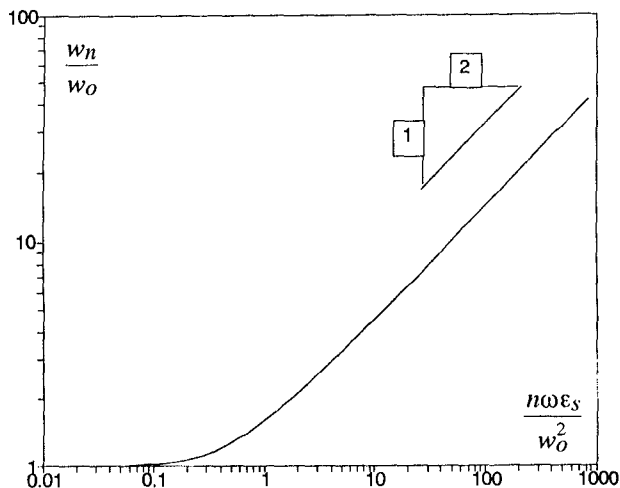


Figure 8: Dependence of w_n on $n\omega\epsilon_s/w_0^2$ in a pure gradient diffusion process with constant diffusivity.

8. References

- Bosman J J** (1982): Concentration measurements under oscillatory water motion. *Delft Hydraulics rep M1695*, part 2.
- Ribberink, J S & A Al-Salem** (1989): Bedforms, near-bed sediment concentrations and sediment transport in simulated regular wave conditions. *Delft Hydraulics Tech Rep no 840*.
- Horikawa K, A Watanabe & S Katori** (1982): Sediment transport under sheet flow condition. *Proc 18th Int Conf Coastal Eng, Capetown*, pp 1335-1352.
- McFetridge, W F & P Nielsen** (1985): Sediment suspension by non-breaking waves over rippled beds. *Tech Rep COEL- 85/005*, Coastal and Oceanographical Eng Dept, Univ of Florida, 132 pp.
- Nadaoka, K, S Ueno, & T Igarashi** (1988): Sediment suspension due to large eddies in the surf zone. *Proc 22nd Int Conf Coastal Eng, Malaga*, pp 1646-1660.
- Nielsen, P** (1983): *Some basic concepts of wave sediment transport*. Series paper 20, Institute of Hydrodynamics and Hydraulic Engineering (ISVA), Technical Univ Denmark.
- Nielsen, P** (1983): Entrainment and distribution of different sand sizes in the same flow. *J Sedimentary Petrology, Vol 53, No 2*, pp 423-428.
- Nielsen, P** (1991): Combined convection and diffusion: A new framework for suspended sediment modelling. *Proc "Coastal Sediments '91"*, Seattle, pp 418-431.
- Nielsen, P** (1992): *Coastal bottom boundary layers and sediment transport*. World Scientific, Singapore, 324 pp.
- Nielsen, P, I A Svendsen & C Staub** (1978): Onshore-offshore sediment transport on a beach. *Proc 16th Int Conf Coastal Eng, Hamburg*, pp 1475-1492.
- van de Graaff, J** (1988): *Sediment concentration due to wave action*. Dr Eng Thesis, Dept of Civil Engineering, Delft University of Technology.